FULL-LENGTH PAPER

A rational approach to selective pharmacophore designing: an innovative strategy for specific recognition of Gsk3β

H. Pradeep · G. K. Rajanikant

Abstract We propose a novel cheminformatics approach that combines structure and ligand-based design to identify target-specific pharmacophores with well-defined exclusion ability. Our strategy includes the prediction of selective interactions, developing structure, and knowledge-based selective pharmacophore models, followed by database screening and molecular docking. This unique strategy was employed in addressing the off-target toxicity of Gsk3β and CDKs. The connections of Gsk3β in eukaryotic cell apoptosis and the extensive potency of Gsk3β inhibitors to block cell death have made it a potential drug-discovery target for many grievous human disorders. Gsk3β is phylogenetically very closely related to the CDKs, such as CDK1 and CDK2, which are suggested to be the off-target proteins of Gsk3β inhibitors. Here, we have employed novel computational approaches in designing the ligand candidates that are potentially inhibitory against Gsk3β, with well-defined the exclusion ability to CDKs. A structure-ligand -based selective pharmacophore was modeled. This model was used to retrieve molecules from the zinc database. The hits retrieved were further screened by molecular docking and protein–ligand interaction fingerprints. Based on these results, four molecules were predicted as selective Gsk3β antagonists. It is anticipated that this unique approach can be extended to investigate any protein–ligand specificity.

Keywords Selective pharmacophore · Gsk3β · CDK1 · CDK2 · Molecular docking

H. Pradeep · G. K. Rajanikant (✉)
Bioinformatics Centre, School of Biotechnology,
National Institute of Technology, Calicut 673601, India
e-mail: rajanikant@nitc.ac.in

Introduction

Herein, we introduce a novel computational screening strategy, which considers both the ligand features and receptor information for the identification of target-specific inhibitors. This rational approach includes deriving energy based pharmacophores [E-pharmacophores] from individual protein and using them to build selective pharmacophores, which are then sequentially employed to screen chemical databases. The selective pharmacophore model ensures that all essential features of each individual protein required for inhibition are conserved and taken into consideration during the sequential screening. Further, it also confirms that the final hits will have all essential features required for the selectivity towards single protein. To the best of our knowledge, this methodology has not been previously described to identify any selective inhibitors. In the present article, this unique strategy has been demonstrated by implementing on the classical example of glycogen synthase kinase 3β (Gsk3β) and cyclin dependent kinases (CDKs) off-target toxicity.

Toxicity is a leading cause of attrition at all stages of the drug development process. Most of the safety-related attrition occurs at the preclinical level, earlier to which designing process might have exacted major portion of both time and money of the pharmaceutical companies [1]. Despite the tremendous advances in the science and technology of drug development, strangely there are no efficient approaches to tackle off-target effects of drugs. The consequences of off-target toxicity are increasing apace, prompting a desperate need of effective strategies against molecular cross-talking. Toxicity of drug is attributed by the molecular features that ensue in molecular cross-talk with different proteins rather than targeted protein. Hence, there is a burgeoning need to develop inhibitors that bind selectively to the

target protein to address the toxicity related attritions [2,3].

Gsk3β is a highly conserved evolutionary serine–threonine kinase. Historically, it was depicted as a central protein required in glycogen metabolism [4]. However, mounting evidence indicates that Gsk3β is a multifunctional enzyme involved in various crucial pathways such as the insulin signaling [5] and the Wnt pathway [6], and plays a crucial role in the synaptic plasticity [7] and memory formation [8]. Most significant functions of this kinase are its role in the phosphorylation of apoptotic regulators and other cell death related factors, thus promoting the cellular degeneration [9,10]. Hence, Gsk3β has emerged as one of the most attractive therapeutic targets for the development of selective antagonists as promising new drugs for numerous debilitating diseases such as Alzheimer's disease, ischemic stroke, chronic inflammatory processes, cancer and diabetes [11–15].

Most of the Gsk3β inhibitors developed thus far often show off-target effects due to serious limitations in their specificity. The low specificity of these inhibitors is due to the fact that the ATP binding site is highly conserved among diverse protein kinases. Even an extremely promising Gsk3β antagonist, can produce off-target effects by inducing changes in protein kinases, especially CDK1 or CDK2. CDK1 and CDK2 are archetypical kinases and central regulators that drive cells through G2 phase and mitosis, the inhibition of these key proteins has negative consequences on cell-cycle progression. As CDKs and Gsk3β belong to the same family of CMGC kinases, they share a high degree of sequence and structural homology [16]. Hence, a strategy should be implemented to develop Gsk3β selective inhibitors which perceptively exclude CDK1 and CDK2. To achieve these goals, we have (1) exploited the energetic analysis of protein–ligand docking to elucidate the key features of proteins/ligand molecular interactions, (2) employed the knowledge-based coherent poses to derive a structure-based pharmacophore for Gsk3β and CDKs, (3) manually developed a selective pharmacophore by the visual analysis of all the three pharmacophores, and (4) applied the selective pharmacophore and virtual screening (VS) protocol to identify selective inhibitors of Gsk3β with the exclusion ability against CDKs (Fig. 1).

Materials and methods

Structure preparation

The crystal structure of Gsk3β (PDB ID: 3GB2, 1Q41), and CDK2 (PDB ID: 3S2P) complexed with their respective antagonists were obtained from Protein Data Bank. Since,
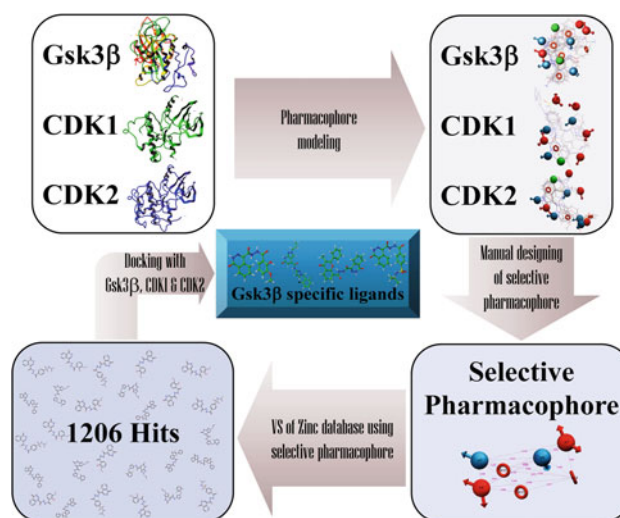

Fig. 1 Pipeline depicting the selective inhibitor designing

the crystal structure of CDK1 is not available we built a homology model from the reported structure of CDK2 and employed in molecular modeling. The 3D structure of protein complexes was prepared using the protein preparation wizard tool (Schrodinger, LLC, 2010); water molecules were deleted, bond orders were assigned, hydrogens were added and metals were treated appropriately when present. Next, the orientation of the side chain structures of Gln and Asn was flipped if necessary to provide the maximum degree of H-bond interactions. The charge state of his residues was optimized. Finally, a restrained minimization of the protein structure was performed using the OPLS force field with backbone atoms being fixed [17].

Prepared protein structures were used to generate Glide scoring grids for the subsequent docking calculations. To each of the crystal structures of protein, a grid box of default size (20 × 20 × 20 Å) was centered on the corresponding active site position. Default parameters were used and no constraints were included during grid generation.

The information of a binding pocket of a protein for its ligand is very important for revealing true binding mechanism and conducting mutagenesis studies [18–21]. The binding pocket consists of a set of residues that have at least one heavy atom with a distance 5.0 Å from any heavy atom of a ligand. Such a criterion was originally used to define the binding pocket of ATP in the Cdk5–Nck5a* complex [22] that has later proved quite useful in identifying functional domains and stimulating the relevant truncation experiments [23]. The similar approach has also been used to define the binding pockets of many other receptor–ligand interactions important for drug design [19,24–27]. Here, the binding pockets were manually defined by either selecting the amino acid residues that span the kinase domain or selecting the ligand present within the crystal structure.

Generation of selective pharmacophore model

Recently developed E-pharmacophore approach of Schrödinger was employed in the construction of these energy-optimized pharmacophores. The E-pharmacophore [28,29] coalesces the ligand and receptor-based techniques. Here, we have used the inhibitor library to probe the pharmacophoric features that are necessary for the selective inhibition of Gsk3β. This method has the advantage of combining pharmacophore perception with protein–ligand energetic terms to rank the importance of pharmacophore features. This combined approach attempts to take a step beyond simple contact scoring, by incorporating structural and energetic information obtained by docking.

The library of 1,500 ligands for each protein was obtained from ChEMBL web site (https://www.ebi.ac.uk/chembldb/) and was used to probe the interaction types and chemically feasible geometries that are involved in the active site and ligand binding. The structures were annotated to expand protonation and tautomeric states using LigPrep [30] and ionization states at pH 7.0 ± 2.0 with Epik [31]. The generated grid files from the prepared receptors of Gsk3β and CDKs were used for the Glide_XP docking calculations. In Glide [32,33], the docking module "write XP descriptor information" option was enabled and rest of the parameters were kept as default. The XP scoring function was used to order the best ranked compounds and the specific interactions like π-cation and π − π stacking. In brief, the docking models of the inhibitors were refined using Glide XP, the Glide XP scoring terms were computed, and the energies were mapped into atoms.

The E-pharmacophore sites were automatically generated with Phase [34], using the default set of six chemical features: H-bond acceptor (A), H-bond donor (D), hydrophobic (H), negative ionizable (N), positive ionizable (P), and aromatic ring (R). In this manner, pharmacophores were derived for each of the proteins, representing Gsk3β, CDK1 and CDK2 and later were evaluated manually for the generation of selective models.

The best pharmacophore hypothesis, AADDRRR was selected based on the careful observations of the feature scores and alignment of ligand structures to the generated hypotheses. The selected 3D pharmacophore hypothesis encompassed the following features: two H-bond acceptors [(A) (pink sphere with two arrows)], two H-bond donors [(D) (pale blue sphere with single arrow)], and three aromatic ring features [(R) (orange ring)].

Pharmacophoric screening

The selective pharmacophore model (AADDRRR) was used as a query for retrieving potential inhibitors from the ZINC chemical database (13 million compounds). Virtual screening was carried out using zincPharmer [35,36] that uses the pharmacophore to efficiently search the ZINC database of fixed conformers for pharmacophore matches. To accomplish the best 3D similarity search, we used constraints that included a maximum of 0.5 RMSD, obeying 15 rotatable bond cutoff and molecular weight range of 180–500 Dalton. The compounds that matched well with the pharmacophoric features of the AADDRRR hypothesis were retrieved as hits and were considered for molecular docking studies.

Docking methodology

Docking study was performed using Glide running on Windows XP. The Glide algorithm estimates a systematic search of positions, orientations, and conformations of the ligand in the enzyme-binding pocket via a series of hierarchical filters. The shape and properties of the receptor are symbolized on a grid by various dissimilar sets of fields that furnish precise scoring of the ligand pose.

The potential hit compounds with lowest RMSD and standard molecular weights were considered for the docking analysis. All the hits were subjected to hydrogen additions, removal of salt, ionization and generation of low-energy ring conformations using LigPrep [37,38]. The tautomers for each of these ligands were generated and optimized. Partial atomic charges were computed using the OPLS-2005 force field. The VS workflow in Maestro was used to dock and to score the lead-like compounds. In the first step, Glide was run in high-throughput virtual screen mode. 10 % of the top-scoring ligands were kept to move onto the Glide Single Precision (SP), stage. 5 % of the top-scoring leads from Glide-SP were retained and docked with Glide XP. Default values were accepted for van der Waals scaling and input partial charges were used. During the docking process, the G-score was used to select the best conformation for each ligand. G-score is based on the ChemScore, but includes a steric-clash term and adds buried polar atoms devised by the Schrodinger to penalize electrostatic mismatches: G-score = 0.065*vdW + 0.130*Coul + Lipo + Hbond + BuryP + RotB + site.

To demonstrate the effectiveness of the described strategy, an additional docking experiment was carried out to compare the selective ability of our method with previously reported computational approaches for the identification of Gsk3β inhibitors. Here, we selected 15 potent ligands reported earlier for Gsk3β inhibition [39–46]. These ligands were prepared using the LigPrep and conformational flexibility was sought through the ConfGen tool of the Schrodinger suite. Finally, the low-energy 3D structures of all the ligands were generated and employed in XP docking into the active sites of Gsk3β, CDK1, and CDK2.
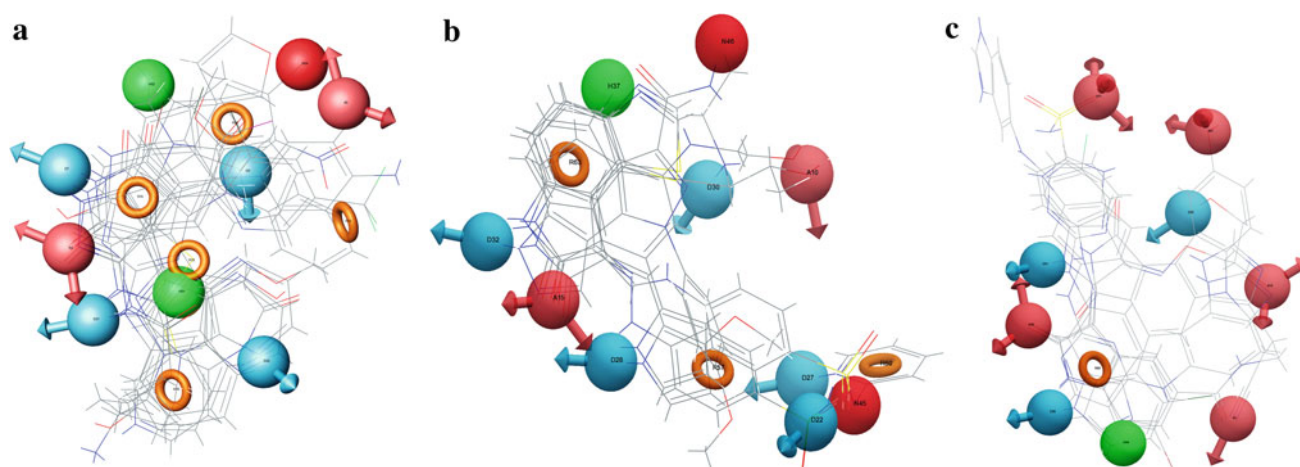
Fig. 2 Comparison of pharmacophoric space of **a** Gsk3β, **b** CDK1 and **c** CDK2

Results and discussion

Generation of selective pharmacophore model

The E-pharmacophore is a unique strategy, which blends the beneficial aspects of structure-based and ligand-based techniques. Mounting evidence indicates the advantage of incorporating protein–ligand interactions over the analysis with conventional ligand information alone. Here, we have used the inhibitor library for each protein to probe the pharmacophoric features that are necessary for the selective inhibition of Gsk3β [47–50]. This method has the advantage of combining pharmacophore perception with protein–ligand energetic terms to rank the importance of pharmacophore features. This protein–ligand based approach attempts to take a step beyond simple contact scoring by incorporating structural and energetic information using the scoring function in glide extra precision (XP).

Overall, 15 pharmacophore sites were predicted for each protein. The pharmacophore hypotheses of Gsk3β, CDK1, and CDK2 were analyzed carefully and as expected the pharmacophore hypotheses exhibited high degree of similarity with each other, especially at the base recognition part of the kinases (ADR of the all pharmacophore models) (Fig. 2). From this, we understand that an ideal pharmacophore should possess these features, in addition to which we have to redact few discriminating features. By careful observation of the protein structure and pharmacophore, we concluded that the addition of donor and aromatic features 5 Å above to the base recognition features would be ideal exclusion strategy. The final hypothesis AADDRRR consists of two H-bond acceptors (A), two H-bond donor (D), and three aromatic ring (R) features. Inter-site distances between each feature are shown in Fig. 3.The H-donor (D7) maps to the carboxylic group of the Asp133, while the H-bond acceptor (A4)

maps to the peptidyl amino group of the Val135, indicating a strong influence on possible inhibition. Two aromatic features (R13 and R15) occupy the hydrophobic cleft in the base recognition site. While the acceptor (A5) and aromatic (R14) features are crucial for selectivity, spans ribose pocket of the active site (Fig. 4). The ribose pocket of the Gsk3β is comparatively wider than both CDK1 and CDK2, hence the former can tolerate bulkier groups at this position when compared to CDKs. Thus, these energetically favorable features encompass the specific interactions required for the selectivity of the Gsk3β protein, and this information should prove helpful in the development of new Gsk3β inhibitors.

Virtual screening

Pharmacophore-based methods have been widely used in virtual screening [48,50–54]. Application of structure-based pharmacophore in VS provides an advantage over the ligand-based pharmacophore approach as it uses the spatial information of the target protein for topological description of ligand–receptor interactions. It also provides an efficient alternative to docking-based VS, while continuing to represent specific ligand–protein interactions. Moreover, recent studies indicated that the structure-based pharmacophore approach provided more detailed information and accuracy in its description of ligand binding than ligand-based methods.

VS was performed to identify possible lead compounds from the zinc database. The zinc chemical database with drug-like compounds consisting of over 13 million structurally diverse small molecules was screened with this query using the zincPharmer tool. A molecule which fits well with the pharmacophoric features, AADDRRR, was retrieved as a hit. Since the active site of Gsk3β is large, the hits may be larger in size and may violate the Lipinski's rule of five.

Fig. 3 Intersite distance in the geometry of the pharmacophore. *Red spheres* with vectors represent acceptor feature, *blue spheres* with vectors represent donor feature and *orange ring* represents aromatic feature
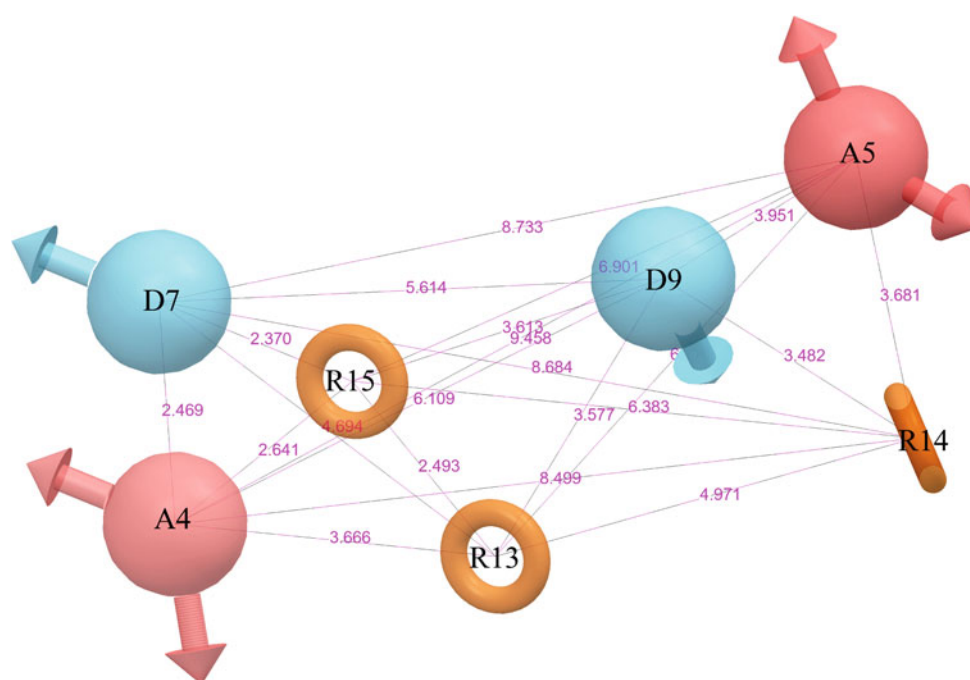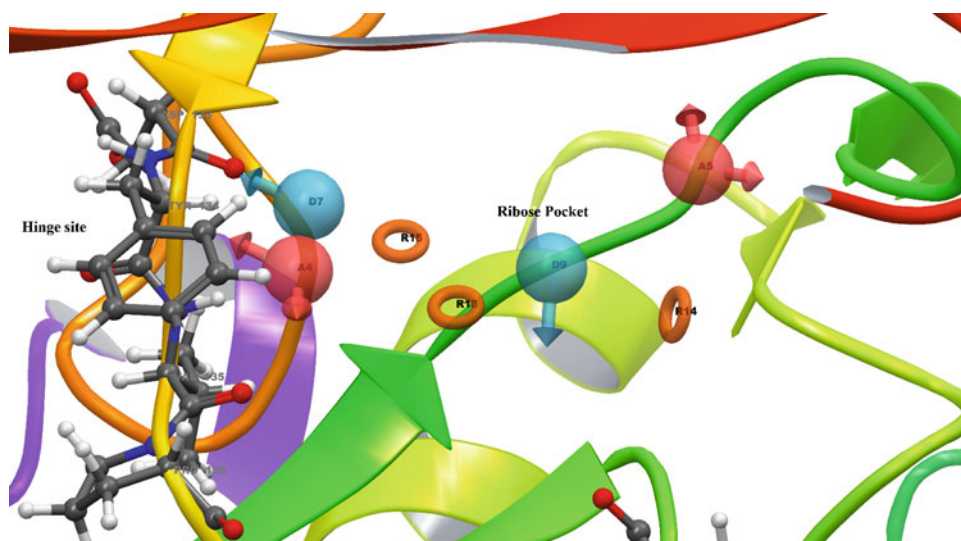

Fig. 4 Pharmacophore model aligned into the active site of the Gsk3β

To avoid possible inappropriate predictions, the molecular weight cutoff of 180–500 dalton range, RMSD of 0.5 and cutoff limit of 15 rotatable bonds filters were applied. Altogether, 3D structural query retrieved 1,206 compounds from the ZINC database.

Docking mode analysis

Molecular docking is a computational technique that tries to predict most desirable conformation of the ligand that fits into the receptor site of the protein. Docking is espe-

cially useful as second step of the virtual screening for the identification of molecules that can fit into the pharmacophore.

To further refine the retrieved hits and also to remove the false positives, VS hits were prepared using LigPrep and docked into the Gsk3β and CDKs using Glide. Further, the low-energy stereoisomers for each structure were generated; ultimately giving rise to 2534 isomers. Docking calculations were carried out using the VS workflow, a docking interface in the Schrödinger software. Finally, the binding modes of ten structures for each protein obtained by docking were ranked

Table 1 Selective hits with their molecular interactions and docking scores

Ligand	Hydrophobic crevice	H-bond	Docking score
(a) Gsk3β			
ZINC60792328	Ile51, Ile62, Val70, Leu132, Leu188 and Val110	Gly65, Lys85, Asp133 and Val135	−10.2
ZINC14239828	Val70, Ala83, Ile62, Val110, Leu132 and leu188	Asp133, Val135 and Gln185	−9.45
ZINC17194074	Lys85, Val70, Ile62, Tyr134, Leu132, Leu188 and Cys199	Asp133, Val135 and Lys183	−9.0
ZINC36621457	Ile51, Val70, Tyr134, Leu188, Cys199 and Val110	Try59, Asp133 and Val135	−8.3
(b) CDK1			
ZINC60792328	Val18, Phe82, Leu83 and Leu135	Ile10 and Leu83	−7.2
ZINC17194074	Lys33, Val18 and Phe80	Leu83	−5.3
ZINC36621457	Val18 and Phe80	Gln132 and Lys89	−3.9
ZINC14239828	Ala31, Val18 and Leu135	Leu83	−2.2
(c) CDK2			
ZINC60792328	Val18 and Lys33	Ile10 and Asp86	−7.4
ZINC14239828	Val49, Ile51 and Try59	Lys18 and Glu81	−6.9
ZINC36621457	Val18, Lys33 and Val18	Asp86 and Lys89	−6.4
ZINC17194074	Val18, Phe80 and Ala31	Lys18 and Leu83	−5.4

a Gsk3β, *b* CDK1, and *c* CDK2

according to the information obtained by different scoring constraints. The binding efficiency of the hits retrieved from docking analysis for Gsk3β is shown in Table 1a, the G-score value is ranging between −8.3 and −10.2. The hits retrieved from docking analysis for CDK1 and CDK2 is shown in Table 1b, c, the G-score value ranges between −2.1 and −7.4. More negative GlideScore value indicates a better interaction of the inhibitor with the target protein. Based on the knowledge of the kinase site requirements and the docking score, the top four structures were chosen as most selective ligands.

The top four hits of Gsk3β (Fig. 5) exhibited all the conventional interactions that are required for the inhibition of kinase activity, viz. interfering with the ATP biding ability of Asp133 and Val135 and hydrophobic interactions with the hydrophobic cleft formed by Lys85, Val70, Ile62, Leu188, Cys199, and Val110. The hinge residues depicted H-bond interactions with ligand and occupy H-donor (D7) and H-bond acceptor (A4) of the pharmacophore. While, hydrophobic cleft maps to the two aromatic features (R13 and R15) of the AADDRRR hypothesis. However, the docking of these ligands to the CDKs protein did not show any of these interactions, suggesting the low affinity of these ligands to the CDK active site (Table 1b, c). By visualizing Fig. 6, we can assume that the aromatic group (R14) faces steric clashes with Gly13, Glu 12, Asn133, Gln132, and Glu163 residues of CDKs, whereas R14 was well tolerated by Gsk3β. Because of the steric clashes, the ligands in the active site of the CDKs tend to disorient, ensuing low affinity of these ligands to the CDK active site.

In order to demonstrate the effectiveness of our approach, we performed the comparative docking analysis on fifteen GSK3β ligands collected from previously reported computational work. All these ligands were employed in docking against GSK3β, CDK1, and CDK2. All 15 ligands showed nearly identical GlideScore for GSK3β, CDK1 and CDK2, suggesting a high affinity of these ligands to the CDKs active site as well (Table 2). In comparison, the evaluation of Glide-Scores of the ligands derived from our approach indicated a greater selectivity towards GSK3β (Table 1).

Many marvelous biological functions of proteins and their profound dynamic mechanisms can be revealed by studying their internal motions [55–58]. Likewise, to accurately identify the ligand-binding pocket [59] and to really understand the interaction of a protein receptor with its ligand, we should consider not only the static structures concerned but also the dynamical information obtained by simulating their internal motions or dynamic process [59–62]. We will make further efforts in this regard in our future study.

Conclusions

Mounting evidence implicate that GSK3β plays an important role in the onset of many grievous human diseases. Recent data have further illustrated the contribution of Gsk3β activity to apoptosis, suggesting that the design and development of selective small molecule inhibitors of Gsk3β may be a good therapeutic option in the treatment of numerous human diseases, associated with apoptosis.

In this study, a new protocol for selective lead identification for Gsk3β has been proposed. The protocol combines both ligand and structure-based approaches. A highly
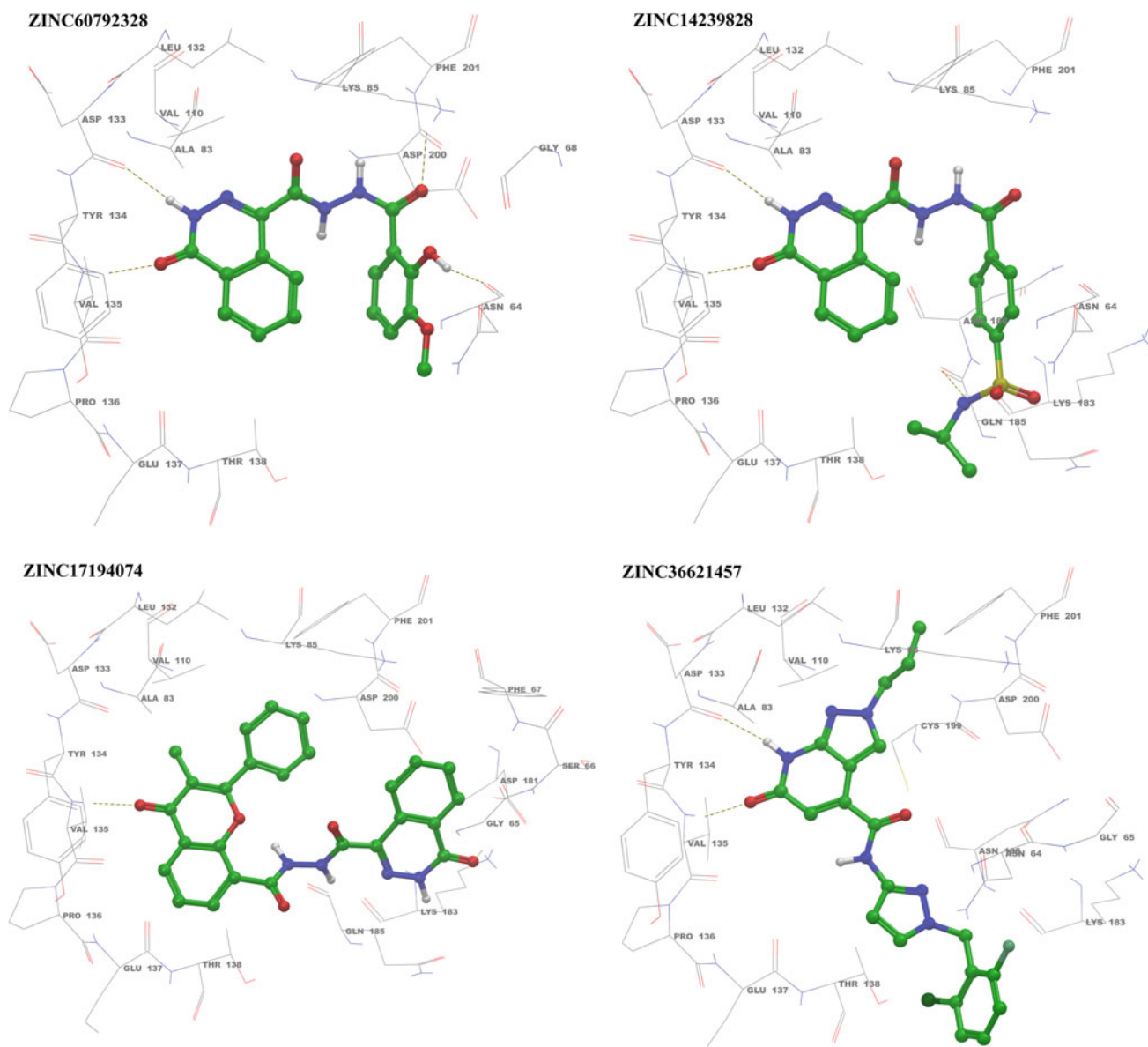
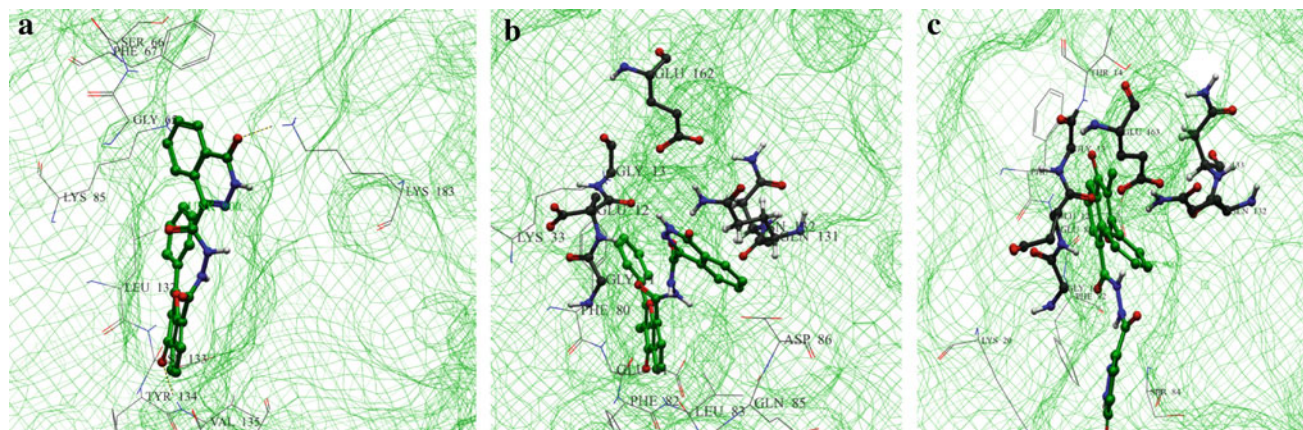**Fig. 5** Docking of selective hits to the active site of GSK3β

Fig. 6 Most selective ligand docked to the active sites of **a** GSK3β, **b** CDK1 and **c** CDK2

Table 2 Previously reported inhibitors of Gsk3β with their docking scores for Gsk3β, CDK1 and CDK2

CHEMBL ID	GlideScore		
	GSK3β	CDK1	CDK2
CHEMBL1081973	−9.80	−9.97	−12.4
CHEMBL1082152	−7.36	−10.6	−11.2
CHEMBL1082153	−11.1	−11.9	−11.2
CHEMBL1099276	−7.50	−6.70	−8.05
CHEMBL1682842	−6.79	−8.18	−8.66
CHEMBL272629	−10.0	−9.74	−9.99
CHEMBL287508	−7.34	−8.52	−8.08
CHEMBL407981	−8.78	−7.66	−8.05
CHEMBL408481	−10.6	−9.36	−10.5
CHEMBL477038	−9.60	−10.1	−10.4
CHEMBL477954	−8.47	−7.91	−8.04
CHEMBL489833	−9.39	−9.33	−7.08
CHEMBL491647	−7.11	−9.20	−9.44
CHEMBL512208	−7.05	−6.01	−6.38
CHEMBL518732	−9.13	−8.51	−9.09

Nearly identical docking scores of the ligands for all three proteins (Gsk3β, CDK1 and CDK2) indicate their equal affinity towards the target proteins
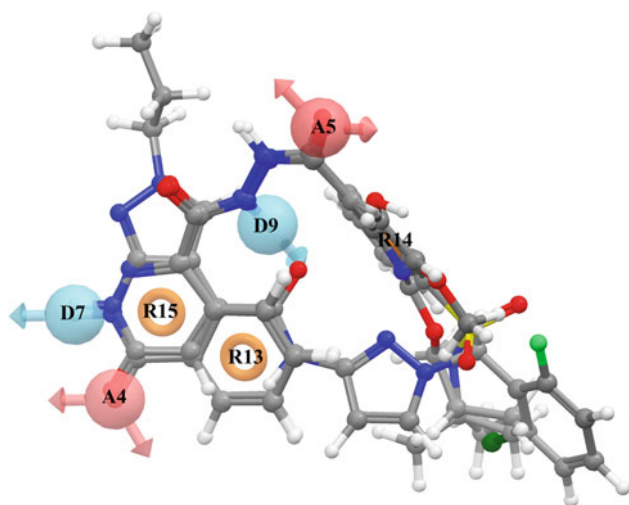
Fig. 7 Alignment of the selective hits with the pharmacophore hypothesis, AADDRRR

potent pharmacophore hypothesis was developed consisting of seven point pharmacophore (AADDRRR): two H-acceptor (A), two H-donor (D), and three aromatic ring features (R). In pharmacophore studies, the spatial alignment of the compounds is usually one of the key steps to obtain meaningful result. Figure 7 shows the good alignment of docked ligands with the pharmacophore. The pharmacophore model was further used to screen potential compounds from the zinc database. The VS process fetched 1,206 ligands as hits,

which were further filtered by docking analysis. Finally, four hits obtained after docking procedure demonstrated better docking score, Glide energy and greater selectivity towards Gsk3β.

In conclusion, unifying the pharmacophore modeling, screening, molecular docking, and manual interpretation approach altogether, we have developed a new methodology to identify selective inhibitors for Gsk3β (Fig. 1). Further, we have delineated the important interactions responsible for binding and selectivity of ligands to the active site more effectively. This protocol may be useful for the identification of specific lead molecules for other potential drug targets as well.

Conflicts of interest The authors report no declarations of interest.

References

1. Kramer JA, Sagartz JE, Morris DL (2007) The application of discovery toxicology and pathology towards the design of safer pharmaceutical lead candidates. Nat Rev Drug Discov 6:636–649. doi:10.1038/nrd2378
2. Lee DU, Jessen B (2012) Off-target immune cell toxicity caused by AG-012986, a pan-CDK inhibitor, is associated with inhibition of p38 MAPK phosphorylation. J Biochem Mol Toxicol 26: 101–108. doi:10.1002/jbt.20415
3. Cao Y, Marks JD, Huang Q, Rudnick SI, Xiong C et al (2012) Single-chain antibody-based immunotoxins targeting Her2/neu: design optimization and impact of affinity on antitumor efficacy and off-target toxicity. Mol Cancer Ther 11: 143–153. doi:10.1158/1535-7163.MCT-11-0519
4. Grimes CA, Jope RS (2001) The multifaceted roles of glycogen synthase kinase 3beta in cellular signaling. Prog Neurobiol 65: 391–426. doi:10.1016/S0301-0082(01)00011-9
5. Liu Y, Tanabe K, Baronnier D, Patel S, Woodgett J et al (2010) Conditional ablation of Gsk-3β in islet beta cells results in expanded mass and resistance to fat feeding-induced diabetes in mice. Diabetologia 53:2600–2610. doi:10.1007/s00125-010-1882-x
6. Zhu Z, Kremer P, Tadmori I, Ren Y, Sun D et al (2011) Lithium suppresses astrogliogenesis by neural stem and progenitor cells by inhibiting STAT3 pathway independently of glycogen synthase kinase 3 beta. PLoS One 6:e23341. doi:10.1371/journal.pone.0023341
7. Peineau S, Bradley C, Taghibiglou C, Doherty A, Bortolotto ZA et al (2008) The role of GSK-3 in synaptic plasticity. Br J Pharmacol 153:S428–437. doi:10.1038/bjp.2008.2
8. Forlenza OV, Torres CA, Talib LL, de Paula VJ, Joaquim HP et al (2011) Increased platelet GSK3B activity in patients with mild cognitive impairment and Alzheimer's disease. J Psychiatr Res 45:220–224. doi:10.1016/j.jpsychires.2010.06.002
9. Linseman DA, Butts BD, Precht TA, Phelps RA, Le SS et al (2004) Glycogen synthase kinase-3beta phosphorylates bax and promotes its mitochondrial localization during neuronal apoptosis. J Neurosci 24: 9993–10002. doi:10.1523/JNEUROSCI.2057-04.2004
10. Morel M, Authelet M, Dedecker R, Brion JP (2010) Glycogen synthase kinase-3beta and the p25 activator of cyclin dependent kinase 5 increase pausing of mitochondria in neurons. Neuroscience 167:1044–1056. doi:10.1016/j.neuroscience.2010.02.077

11. Mendes CT, Mury FB, Sá Moreira E , de Alberto FL, Forlenza OV et al (2009) Lithium reduces Gsk3b mRNA levels: implications for Alzheimer Disease. Eur Arch Psychiatry Clin Neurosci 259:16–22. doi:10.1007/s00406-008-0828-5

12. Zhai P, Sadoshima J (2012) Glycogen synthase kinase-3β controls autophagy during myocardial ischemia and reperfusion. Autophagy 8:138–139. doi:10.4161/auto.8.1.18314

13. Hofmann C, Dunger N, Schölmerich J, Falk W, Obermeier F (2010) Glycogen synthase kinase 3-β: a master regulator of toll-like receptor-mediated chronic intestinal inflammation. Inflamm Bowel Dis 16:1850–1858. doi:10.1002/ibd.21294

14. Schütz SV, Schrader AJ, Zengerling F, Genze F, Cronauer MV et al (2011) Inhibition of glycogen synthase kinase-3β counteracts ligand-independent activity of the androgen receptor in castration resistant prostate cancer. PLoS One 6:e25341. doi:10.1371/journal.pone.0025341

15. Jolivalt CG, Calcutt NA, Masliah E (2012) Similar pattern of peripheral neuropathy in mouse models of type 1 diabetes and Alzheimer's disease. Neuroscience 202:405–412. doi:10.1016/j.neuroscience.2011.11.032

16. Ko HW, Kim EY, Chiu J, Vanselow JT, Kramer A et al (2010) A hierarchical phosphorylation cascade that regulates the timing of PERIOD nuclear entry reveals novel roles for proline-directed kinases and GSK-3beta/SGG in circadian clocks. J Neurosci 30:12664–12675. doi:10.1523/JNEUROSCI.1586-10.2010

17. Teli MK, Rajanikant GK (2011) Pharmacophore generation and atom-based 3D-QSAR of novel quinoline-3-carbonitrile derivatives as Tpl2 kinase inhibitors. J Enzyme Inhib Med Chem 26:1–13. doi:10.3109/14756366.2011.603128

18. Schnell JR, Chou JJ (2008) Structure and mechanism of the M2 proton channel of influenza A virus. Nature 451:591–595. doi:10.1038/nature06531

19. Huang RB, Du QS, Wang CH, Chou KC (2008) An in-depth analysis of the biological functional studies based on the NMR M2 channel structure of influenza A virus. Biochem Biophys Res Commun 377:1243–1247. doi:10.1016/j.bbrc.2008.10.148

20. Du QS, Huang RB, Wang CH, Li XM, Chou KC (2009) Energetic analysis of the two controversial drug binding sites of the M2 proton channel in influenza A virus. J Theor Biol 259:159–164. doi:10.1016/j.jtbi.2009.03.003

21. Chou KC (2004) Structural bioinformatics and its impact to biomedical science. Curr Med Chem 11:2105–2134. doi:10.1234/12345678

22. Chou KC, Watenpaugh KD, Heinrikson RL (1999) A model of the complex between cyclin-dependent kinase 5 and the activation domain of neuronal Cdk5 activator. Biochem Biophys Res Commun 259:420–428. doi:10.1006/bbrc.1999.0792

23. Zhang J, Luan CH, Chou KC, Johnson GV (2002) Identification of the N-terminal functional domains of Cdk5 by molecular truncation and computer modeling. Proteins 48:447–453. doi:10.1002/prot.10173

24. Chou KC, Wei DQ, Zhong WZ (2003) Binding mechanism of coronavirus main proteinase with ligands and its implication to drug design against SARS. Biochem Biophys Res Commun 308:148–151. doi:10.1016/S0006-291X(03)01342-1

25. Wang SQ, Du QS, Chou KC (2007) Study of drug resistance of chicken influenza A virus (H5N1) from homology-modeled 3D structures of neuraminidases. Biochem Biophys Res Commun 354:634–640. doi:10.1016/j.bbrc.2006.12.235

26. Du QS, Sun H, Chou KC (2007) Inhibitor design for SARS coronavirus main protease based on "distorted key theory". Med Chem 3:1–6. doi:10.2174/157340607779317616

27. Housaindokht MR, Bozorgmehr MR, Bahrololoom M (2008) Analysis of ligand binding to proteins using molecular dynamics simulations. J Theor Biol 254:294–300. doi:10.1016/j.jtbi.2008.04.036

28. Salam NK, Nuti R, Sherman W (2009) Novel method for generating structure-based pharmacophores using energetic analysis. J Chem Inform Model 49:2356–2368. doi:10.1021/ci900212v

29. Loving K, Salam NK, Sherman W (2009) Energetic analysis of fragment docking and application to structure-based pharmacophore hypothesis generation. J Comput Aid Mol Des 23:541–554. doi:10.1007/s10822-009-9268-1

30. Schrödinger (2011) LigPrep, version 2.5. Schrödinger, LLC, New York

31. Shelley JC, Cholleti A, Frye LL, Greenwood JR, Timlin MR et al (2007) Epik: a software program for pK a prediction and protonation state generation for drug-like molecules. J Comput Aid Mol Des 21:681–691. doi:10.1007/s10822-007-9133-z

32. Friesner RA, Banks JL, Murphy RB, Halgren TA, Klicic JJ et al (2004) Glide: a new approach for rapid, accurate docking and scoring. 1. Method and assessment of docking accuracy. J Med Chem 47:1739–1749. doi:10.1021/jm0306430

33. Halgren TA, Murphy RB, Friesner RA, Beard HS, Frye LL et al (2011) Glide: a new approach for rapid, accurate docking and scoring. 2. Enrichment factors in database screening. J Med Chem 47:1750–1759. doi:10.1021/jm030644s

34. Dixon SL, Smondyrev AM, Rao SN (2006) PHASE: a novel approach to pharmacophore modeling and 3D database searching. Chem Biol Drug Des 67:370–372. doi:10.1111/j.1747-0285.2006.00384.x

35. Koes DR, Camacho CJ (2011) Pharmer: efficient and exact pharmacophore search. J Chem Inf Model 51:1307–1314. doi:10.1021/ci200097m

36. Irwin JJ, Shoichet BK (2005) ZINC-a free database of commercially available compounds for virtual screening. J Chem Inf Model 45:177–182. doi:10.1021/ci049714

37. Nair SB, Teli MK, Pradeep H, Rajanikant GK (2012) Computational identification of novel histone deacetylase inhibitors by docking based QSAR. Comput Biol Med 42:697–705. doi:10.1016/j.compbiomed.2012.04.00

38. Teli MK, Rajanikant GK (2012) Identification of novel potential HIF-prolyl hydroxylase inhibitors by in silico screening. Mol Divers 16:193–202. doi:10.1007/s11030-011-9338-x

39. Coffman K, Brodney M, Cook J, Lanyon L, Pandit J et al (2011) 6-Amino-4-(pyrimidin-4-yl)pyridones: novel glycogen synthase kinase-3β inhibitors. Bioorg Med Chem Lett 21:1429–1433. doi:10.1016/j.bmcl.2011.01.017

40. Gong L, Hirschfeld D, Tan YC, Heather Hogg J, Peltz G et al (2010) Discovery of potent and bioavailable GSK-3beta inhibitors. Bioorg Med Chem Lett 20:1693–1696. doi:10.1016/j.bmcl.2010.01.038

41. Kang NS, Lee GN, Kim CH, Bae MA, Kim I et al (2009) Identification of small molecules that inhibit GSK-3beta through virtual screening. Bioorg Med Chem Lett 19:533–537. doi:10.1016/j.bmcl.2008.10.120

42. Rochais C, Duc NV, Lescot E, de Oliveira Santos JS, Bureau R et al (2009) Synthesis of new dipyrrolo- and furopyrrolopyrazinones related to tripentones and their biological evaluation as potential kinases (CDKs1-5, GSK-3) inhibitors. Eur J Med Chem 44:708–716. doi:10.1016/j.ejmech.2008.05.011

43. Rouse MB, Seefeld MA, Leber JD, McNulty KC, Sun L et al (2009) Aminofurazans as potent inhibitors of AKT kinase. Bioorg Med Chem Lett 19:1508–1511. doi:10.1016/j.bmcl.2009.01.002

44. Gaisina IN, Gallier F, Ougolkov AV, Kim KH, Kurome T et al (2009) From a natural product lead to the identification of potent and selective benzofuran-3-yl-(indol-3-yl)maleimides as glycogen synthase kinase 3beta inhibitors that suppress proliferation and survival of pancreatic cancer cells. J Med Chem 52:1853–1863. doi:10.1021/jm801317h

45. Kim HJ, Choo H, Cho YS, No KT, Pae AN (2008) Novel GSK-3beta inhibitors from sequential virtual screening. Bioorg Med Chem 16:636–643. doi:10.1016/j.bmc.2007.10.047

46. Taha MO, Bustanji Y, Al-Ghussein MA, Mohammad M, Zalloum H (2008) Pharmacophore modeling, quantitative structure-activity relationship analysis, and in silico screening reveal potent glycogen synthase kinase-3beta inhibitory activities for cimetidine, hydroxychloroquine, and gemifloxacin. J Med Chem 51:2062–2077. doi:10.1021/jm7009765

47. Liao QH, Gao QZ, Wei J, Chou KC (2011) Docking and molecular dynamics study on the inhibitory activity of novel inhibitors on epidermal growth factor receptor (EGFR). Med Chem 7:24–31. doi:10.2174/157340611794072698

48. Wei J, Qu W, Ye Y, Gao Q (2010) 3D pharmacophore based virtual screening of A 2A adenosine receptor antagonists. Protein Pept Lett 17:332–339. doi:10.2174/092986610790780260

49. Zhang T, Wei DQ, Chou KC (2012) A pharmacophore model specific to active site of CYP1A2 with a novel molecular modeling explorer and CoMFA. Med Chem 8:198–207. doi:10.2174/157340612800493601

50. Sirois S, Wei DQ, Du Q, Chou KC (2004) Virtual screening for SARS-CoV protease based on KZ7088 pharmacophore points. J Chem Inf Comput Sci 44:1111–1122. doi:10.1021/ci034270n

51. Bi J, Yang H, Yan H, Song R, Fan J (2011) Knowledge-based virtual screening of HLA-A*0201-restricted CD8+ T-cell epitope peptides from herpes simplex virus genome. J Theor Biol 281:133–139. doi:10.1016/j.jtbi.2011.04.018

52. Singh V, Somvanshi P (2010) Toward the virtual screening of potential drugs in the homology modeled NAD+ dependent DNA ligase from *Mycobacterium tuberculosis*. Protein Pept Lett 17:269–276. doi:10.2174/092986610790225950

53. Wang SQ, Du QS, Zhao K, Li AX, Wei DQ et al (2007) Virtual screening for finding natural inhibitor against cathepsin-L for SARS therapy. Amino Acids 33:129–135. doi:10.1007/s00726-006-0403-1

54. Hanumanthappa P, Teli MK, Krishnamurthy RG (2012) Generation of pharmacophore and atom based 3D-QSAR model of novel isoquinolin-1-ones and quinazolin-4-ones as potent inhibitors of TNFα. Med Chem 8:436–451

55. Chou KC (1989) Low-frequency resonance and cooperativity of hemoglobin. Trends Biochem Sci 14:212–213. doi:10.1016/0968-0004(89)90026-1

56. Chou KC, Mao B (1988) Collective motion in DNA and its role in drug intercalation. Biopolymers 27:1795–1815. doi:10.1002/bip.360271109

57. Chou KC, Zhang CT, Maggiora GM (1994) Solitary wave dynamics as a mechanism for explaining the internal motion during microtubule growth. Biopolymers 34:143–153. doi:10.1002/bip.360340114

58. Chou KC (1988) Low-frequency collective motion in biomacromolecules and its biological functions. Biophys Chem 30:3–48. doi:10.1016/0301-4622(88)85002-6

59. Li XB, Wang SQ, Xu WR, Wang RL, Chou KC (2011) Novel inhibitor design for hemagglutinin against H1N1 influenza virus by core hopping method. PLoS One 6:e28111. doi:10.1371/journal.pone.0028111

60. Wang JF, Gong K, Wei DQ, Li YX, Chou KC. (2009) Molecular dynamics studies on the interactions of PTP1B with inhibitors: from the first phosphate-binding site to the second one. Protein Eng Des Sel 22:349–355. doi:10.1093/protein/gzp012

61. Li J, Wei DQ, Wang JF, Yu ZT, Chou KC (2012) Molecular dynamics simulations of CYP2E1. Med Chem 8:208–221. doi:10.2174/157340612800493692

62. Liu XY, Wang RL, Xu WR, Tang LD, Wang SQ et al (2011) Docking and molecular dynamics simulations of peroxisome proliferator activated receptors interacting with pan agonist sodelglitazar. Protein Pept Lett 18:1021–1027. doi:10.2174/092986611796378701